Optical spectra of Dy^{3+} in KY$_3$F$_{10}$ and LiLuF$_4$ crystalline fibers

Stefano Bigotta [a,*], M. Tonelli [a], E. Cavalli [b], A. Belletti [b]

[a] NEST-CNR, Dipartimento di Fisica, Università di Pisa, Largo B. Pontecorvo 3, 56127 Pisa, Italy
[b] Dipartimento di Chimica Generale ed Inorganica, Chimica Analitica e Chimica Fisica, Università di Parma, Viale Usberti 17/a, 43100 Parma, Italy

ARTICLE INFO

ABSTRACT

Visible optical properties of two crystalline fibers (KY$_3$F$_{10}$ and LiLuF$_4$) doped with Dy^{3+} have been investigated. In particular, the room-temperature absorption spectra have been analyzed using the Judd–Ofelt theory and the intensity parameters have been obtained. A criterion suitable for determining the proper choice of the dopant composition to tailor the luminescence properties of the crystals is proposed.

1. Introduction

Oxide and fluoride lattices activated with Dy^{3+} present intense luminescence bands in the blue and yellow spectral regions, which make them attractive for applications in the phosphor and solid-state laser technologies [1,2]. The device potentialities of these materials strongly depend on efficiencies of the two involved emission channels, both originating in the ^{4}F$_{9/2}$ excited level. In this connection, it has been observed that the relative intensity of the blue ^{4}F$_{9/2} \rightarrow {}^6$H$_{15/2}$ and of the yellow ^{4}F$_{9/2} \rightarrow {}^6$H$_{13/2}$ transition can be significantly different in different lattices. In some cases, it has been possible to modulate the emitted light by suitably varying the composition of the host, allowing, for example, the realization of interesting white-emitting phosphors [3,4]. The Judd–Ofelt (J–O) analysis of the room-temperature absorption spectra [5,6] allows the determination of probabilities of the radiative transitions in a given host lattice and the estimation of their efficiencies through the comparison with the experimental results. This approach has been extensively applied in the characterization of materials activated with the most common laser ions like Nd^{3+}, Er^{3+}, etc., but only in a limited number of cases of Dy^{3+}-doped compounds. We have then decided to examine a series of these compounds using this procedure to reveal the presence of systematic behaviors useful

for understanding the relations between spectroscopic and structural properties on one hand and to verify the possibility of obtaining materials with suitable emission properties on the other. To date, fluorides have been investigated as host materials for the dysprosium ion mainly to develop NIR laser rather than visible-emitting media [7]. Nevertheless, in a paper concerning Dy^{3+} in BaY$_2$F$_8$ (BYF), we have evidenced some interesting peculiarities with respect to the more extensively investigated oxide lattices [8]. For this reason, we have decided to extend our studies to other fluorides, and in this paper we present results obtained for Dy^{3+}-doped KY$_3$F$_{10}$ (KYF) and LiLuF$_4$ (LiLuF) crystalline fibers.

2. Experimental

Single-crystal fibers of KYF and LiLuF containing 1% and 5% of Dy^{3+}, grown by means of the μ-pulling down method [9], have been provided by Kyoung Jin Kim and Tsuguo Fukuda (IMRAM, Tohoku University). The structure of KYF is cubic, space group Fm$\bar{3}$m with cell parameter $a = 11.553$ Å, [10], that of LiLuF is tetragonal, the space group being I4$_1$ and the cell parameters $a = b = 5.167$ Å and $c = 10.375$ Å [11]. Room-temperature absorption spectra were measured with a spectroscopic system equipped with a 300 W halogen lamp fitted with a 0.25 m Spex monochromator as source, and a 1.26 m Spex monochromator with a RCA C31034 photomultiplier or a PbS NEP cell to analyze and detect the output radiation.

* Corresponding author. Tel.: +39 050 2214536; fax: +39 050 221 4333.
E-mail address: bigotta@df.unipi.it (S. Bigotta).
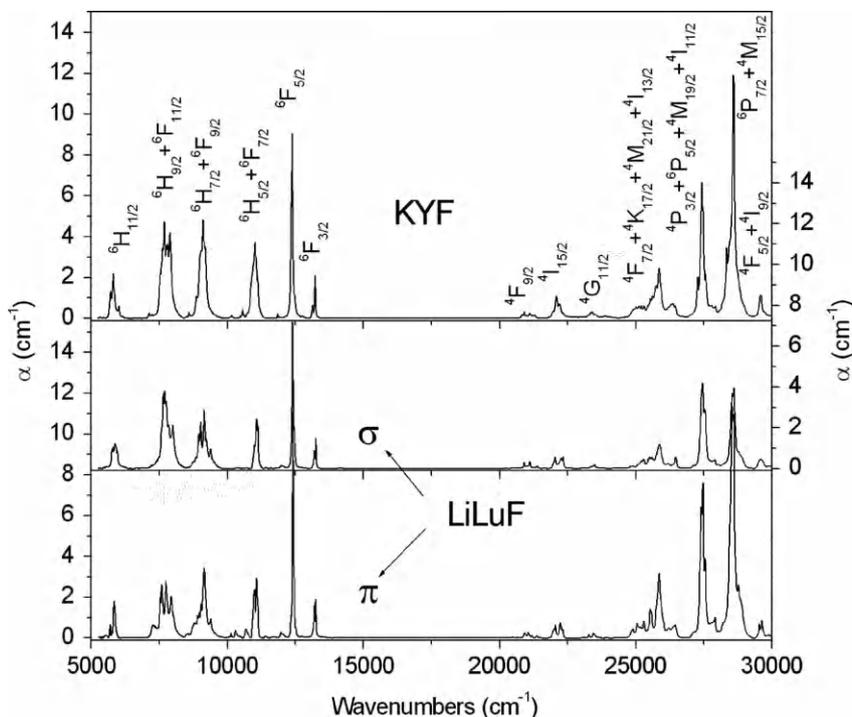
Fig. 1. Room-temperature absorption spectra of 5% Dy^{3+}-doped KYF and LiLuF.

The luminescence spectra in the visible region (440–830 nm) were measured using a 5 W diode led emitting at 385 nm. The luminescence was mechanically chopped and focussed by a lens of 75 mm focal length on the input slit of a 1/3 m monochromator equipped with a 1200 groove/mm grating. The fluorescence was observed perpendicularly to the exciting beam to reduce pump spurious scattering and a suitable filter and a Glan-Thompson polarizer were put in front of the monochromator. The signal was detected by a Hamamatsu R1464 photomultiplier and processed by a lock-in amplifier. The resolution of the fluorescence spectra was better than 0.1 nm. All the polarized spectra were normalized relatively to the absorbed power and the spectra have been corrected for the spectral response of the system using a blackbody source at 3000 K.

For the measurement of the luminescence decay curves, the sample was excited at 355 nm using a pulsed Nd:YAG laser (Quanta System model SYL 202); the emission was isolated by means of a Hilger–Watts Model D330 double monochromator and detected with a Hamamatsu R943-022 photomultiplier connected to a LeCroy 9410 transient digitizer. The samples were cooled by means of an Air Products Displex DE 202 or a Galileo Vacuum Tech Model K1 closed-cycle cryostat.

3. Results and discussion

3.1. Absorption spectra and J–O analysis

The room-temperature absorption spectra of Dy:KYF and Dy:LiLuF are shown in Fig. 1. They are composed of multiplets assigned to the transition from the $^6I_{15/2}$ ground state to the lower excited manifolds of the $4f^9$ electronic configuration of the Dy^{3+} ion. In the case of LiLuF, tetragonal, they are significantly polarized, the π ($E\|c$) bands being in most cases more intense than the σ ($E\perp c$) ones. The spectra have been analyzed in the framework of the J–O Theory. The oscillator strengths of the

absorption transitions have been carefully determined and fitted on the basis of the J–O parametrization scheme [5,6] after subtraction of the magnetic dipole contribution for the $^4I_{15/2}\leftarrow$ $^6H_{15/2}$, $^4I_{13/2}\leftarrow^6H_{15/2}$ and $^4K_{17/2}\leftarrow^6H_{15/2}$ transitions. These contributions are small and not reported here. The reduced matrix elements were taken from Jayasankar and Rukmini [12], and the value of the refractive index was assumed to be $n = 1.50$ in the case of KYF and $n = 1.45$ in that of LiLuF [13]. The evaluated intensity parameters are reported in Table 1, together with the observed and calculated oscillator strengths. The rms deviations, also reported, are of the expected order of magnitude (10–30%), related to the intrinsic uncertainty of the J–O model. The spontaneous emission probabilities and the radiative branching ratios for the transitions from the $^4F_{9/2}$ state to the lower ones have been estimated using the calculated intensity parameters and the reduced matrix elements reported by Jayasankar and Rukmini [12]. They are reported in Table 2, in which we also report the radiative lifetime of the emitting level and its experimental value, as well as the calculated and measured ratio between the yellow and the blue emission. In Table 3, we have compared the calculated J–O parameters and lifetimes with those reported for other crystals activated with Dy^{3+}. On the basis of this comparison we can conclude that:

1. In both KYF and LiLuF, the values of Ω_2 are rather low and similar to those reported for the Nd^{3+}-doped crystals [13]. We point out that this parameter directly depends on the intensity of the hypersensitive transitions [14], and that among the observable optical features of the Dy^{3+}-doped materials only the $^6F_{11/2}\leftarrow^6H_{15/2}$ absorption transition ($\Delta L = 2$, $\Delta S = 0$) is hypersensitive.

2. Inspection of Table 5 of Ref. [12] reveals that the intensity of the $^4F_{9/2}\rightarrow^6H_{13/2}$ band depends much more on the Ω_2 and Ω_6 intensity parameters than on the Ω_4 one, because the values of the reduced matrix elements of rank 2 and 6 for this transition are 0.0512 and 0.0573, respectively, whereas that of rank 4 is

Table 1
Experimental and calculated oscillator strengths (P) of Dy^{3+} in KYF and LiLuF.

Excited state	KYF			LiLuF		
	Barycentre (cm^{-1})	P_{exp} (10^6)	P_{calc} (10^6)	Barycentre (cm^{-1})	P_{exp} (10^6)	P_{calc} (10^6)
$^6H_{11/2}$	5829	0.57	0.66	5857	0.44	0.48
$^6H_{9/2}+^6F_{11/2}$	7748	2.58	2.56	7754	2.13	2.12
$^6H_{7/2}+^6F_{9/2}$	9096	1.94	1.88	9116	1.08	1.08
$^6F_{7/2}$	10865	1.30	1.39	10690	0.73	0.87
$^6F_{5/2}$	12830	0.99	0.63	12399	0.67	0.41
$^6F_{3/2}$	13208	0.15	0.12	13226	0.14	0.08
$^4F_{9/2}$	21040	0.12	0.11	21055	0.09	0.07
$^4I_{15/2}$	22190	0.26	0.24	22178	0.18	0.17
$^4F_{7/2}+^4K_{17/2}+^4M_{21/2}+^4I_{13/2}$	25716	1.20	1.33	25731	0.93	0.83
$^4P_{7/2}+^6P_{5/2}+^4M_{19/2}+^4I_{11/2}$	27470	1.17	1.01	27509	1.19	0.64
$^6P_{7/2}+^4M_{15/2}$	28562	2.37	2.52	28592	1.28	1.25
$^4F_{5/2}+^4I_{9/2}$	29664	0.22	0.10	29651	0.13	0.07
Intensity parameters	$\Omega_2 = 1.55 \times 10^{-20}$ cm^2 $\Omega_4 = 1.81 \times 10^{-20}$ cm^2 $\Omega_6 = 1.63 \times 10^{-20}$ cm^2 RMS $= 1.59 \times 10^{-7}$ %RMS $= 14.9$			$\Omega_2 = 2.04 \times 10^{-20}$ cm^2 $\Omega_4 = 0.91 \times 10^{-20}$ cm^2 $\Omega_6 = 1.09 \times 10^{-20}$ cm^2 RMS $= 2.14 \times 10^{-7}$ %RMS $= 28.5$		

The Judd–Ofelt parameters, Ω_λ, the RMS and the percent errors are also tabulated.

Table 2
Calculated spontaneous emission probabilities A and radiative branching ratios β for the $^4F_{9/2}$ emitting level of Dy^{3+} in KYF and LiLuF.

Final state	KYF		LiLuF	
	A (s^{-1})	β	A (s^{-1})	β
$^6F_{5/2}$	2	0.005	2	0.006
$^6F_{7/2}$	3	0.008	2	0.005
$^6H_{5/2}$	2	0.006	1	0.004
$^6H_{7/2}$	0	0.000	0	0.000
$^6F_{9/2}$	4	0.012	2	0.008
$^6F_{11/2}$	8	0.021	6	0.020
$^6H_{9/2}$	7	0.018	5	0.016
$^6H_{11/2}$	18	0.048	17	0.060
$^6H_{13/2}$	218	0.598	186	0.654
$^6H_{15/2}$	103	0.284	65	0.228
Decay time	$\tau = 2.7$ ms (calc.) $\tau = 440$ μs (exp.)		$\tau = 3.5$ ms (calc.) $\tau = 582$ μs (exp.)	
Y/B ratio	2.12 (calc.) 0.84 (exp.)		2.86 (calc.) 1.09 (exp.)	

only 0.0172. At variance, the intensity of the $^4F_{9/2} \rightarrow ^6H_{15/2}$ transition depends only on the Ω_6 parameter, since the corresponding reduced matrix element has value 0.0303, whereas those of rank 2 and 4 are practically zero. The other emission transitions originating in the $^4F_{9/2}$ are by far less intense, consistently with the very low values of the related reduced matrix elements. From these considerations, we have to expect that when the Ω_2 value increases: (i) the total emission probability from $^4F_{9/2}$ should increase; (ii) the yellow to blue (Y/B) intensity ratio should also increase and (iii) the radiative lifetime and consequently the experimental decay time should decrease. Moreover, the yellow emission should always be more intense than the blue one, at least by a factor of 1.9, corresponding to the ratio between the reduced matrix elements of rank 4.

Concluding, the Ω_2 parameter strongly influences the luminescence properties of the Dy^{3+}-doped materials despite the involved emission transitions are not hypersensitive. In both fluorides under investigation, the relatively low values of Ω_2 should then

result in radiative lifetimes of the order of the milliseconds and in relatively low values of the Y/B intensity ratios, as evidenced in Table 2.

3.2. Emission spectra and decay times measurements

The room-temperature emission spectra of the investigated compounds have been measured upon LED excitation at 385 nm. They are shown in Fig. 2. The intensities of the $^4F_{9/2} \rightarrow ^6H_{15/2}$ blue and $^4F_{9/2} \rightarrow ^6H_{13/2}$ yellow bands are comparable, in qualitative agreement with the low value of the Ω_2 parameter, as discussed in the previous section. It can in fact be pointed out that in Dy^{3+}-doped compounds presenting relatively high values of the Ω_2 parameter (see Table 3 and related references), the blue emission is much less intense than the yellow one. From a quantitative point of view, however, the calculated Y/B intensity ratios are roughly 2.5 times larger (cfr. Table 2) than the corresponding experimental values obtained after integration of the emitted intensities. In this circumstance in conclusion, the J–O approach tends to overestimate the relative intensity of the yellow emission with respect to that of the blue one.

The decay profiles of 1% doped Dy:KYF and Dy:LiLuF have been measured at 575 nm as a function of the temperature. As representative examples, the 298 K curves are shown in Figs. 3 and 4. They are always non-exponential and cannot be reproduced using equations related to simple energy transfer models, indicating that different non-radiative processes are active even at relatively low-doping levels. Different cross-relaxation mechanisms with different temperature dependences can in fact contribute to the depopulation of the emitting level [20]:

$^4F_{9/2}, \ ^6H_{15/2} \rightarrow \ ^4F_{3/2}, \ ^6F_{11/2}$ (nearly resonant)

$^4F_{9/2}, \ ^6H_{15/2} \rightarrow \ ^6H_{5/2}, \ ^6H_{5/2}$ (phonon assisted)
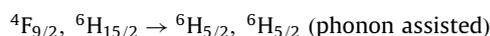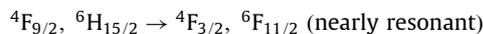
In addition, pairing or clustering effects cannot be excluded, that could result in short range interactions further affecting the transfer rates. In this situation, we have retained it appropriate to estimate the average values of the decay times by the integral method [21]:

$$\tau_{av} = \frac{\int I(t)t\,dt}{\int I(t)\,dt} \tag{1}$$

Table 3
Comparison between the intensity parameters and the radiative lifetimes of the title compounds and other Dy^{3+}-activated crystals.

	Ω_2 ($\times 10^{-20}$ cm^2)	Ω_4 ($\times 10^{-20}$ cm^2)	Ω_6 ($\times 10^{-20}$ cm^2)	$\tau_{rad}(^4F_{9/2})$ (μs)	Reference
KYF	1.55	1.81	1.63	2700	This work
LiLuF	2.04	0.91	1.09	3500	This work
BaY_2F_8	1.52	2.33	3.67	1480	[8]
YVO_4	6.59	3.71	1.74	440	[15]
$YAl_3(BO_3)_4$	10.8	2.05	3.28	460	[16]
$KGd(WO_4)_2$	15.3	3.05	2.01	160	[17]
$KY(WO_4)_2$	23.2	3.33	2.36	166	[18]
$CaMoO_4$	26.6	2.89	1.79	177	[19]
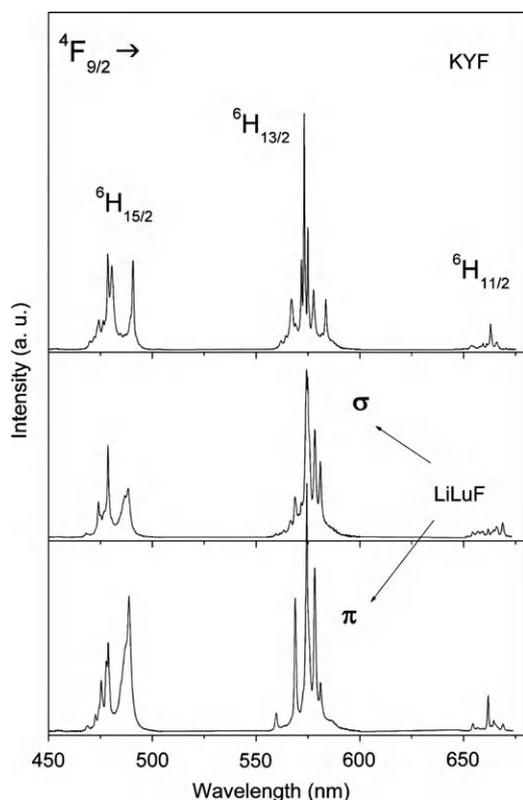
Fig. 2. Room-temperature emission spectra of 1% Dy^{3+}-doped KYF and LiLuF.
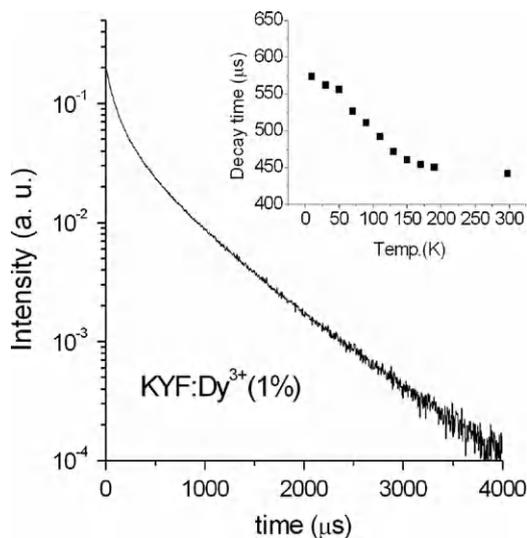
Fig. 3. Decay profile of the room-temperature emission from the $^4F_{9/2}$ level of 1% Dy^{3+}-doped KYF. In the inset: temperature dependence of the decay times.
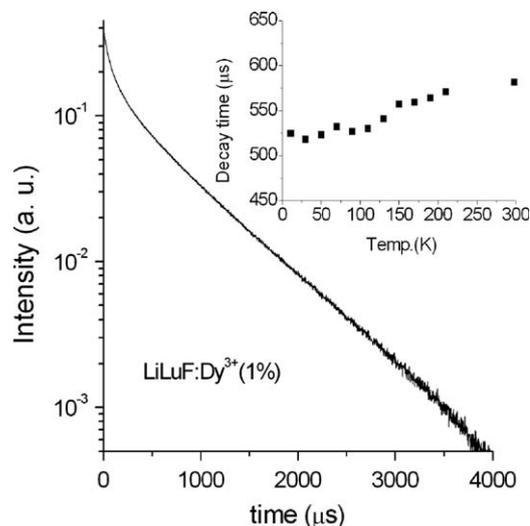
Fig. 4. Decay profile of the room-temperature emission from the $^4F_{9/2}$ level of 1% Dy^{3+}-doped LiLuF. In the inset: temperature dependence of the decay times.

where $I(t)$ is the emission intensity at time t. The decay time of Dy:KYF, shown in the inset of Fig. 3, decreases with the temperature increasing from a value of 575 μs at 10 K to a value of 440 μs at 298 K, whereas that of Dy:LiLuF increases from 525 μs at 10 K to 582 μs at 298 K (inset of Fig. 4). It has to be observed that in most cases the decay time of the $^4F_{9/2}$ emitting level of Dy^{3+}-doped materials slightly increases with the temperature [8,17,22]. Kaminskii et al. [17] ascribe this behavior to the fact that some approximations intrinsic of the Judd–Ofelt approach are not fulfilled in practice, in particular those affirming on one hand that the population of the Stark levels of the initial manifold of a J→J' channel should be the same, and on the other that the probabilities of all inter-Stark electric dipole transitions should be equal. Dominiak-Dzik et al. [22] take also into consideration the possibility of thermal population of the next upper lying $^4I_{15/2}$ level, whose radiative lifetime is significantly longer than that of $^4F_{9/2}$. As a matter of fact, however, the reasons of such an increase are still to be fully understood. In this context, we can point out that the measured decay times are much shorter than the calculated lifetimes, which are of the order of 2–3 ms. This large discrepancy can have two origins: first, the J–O theory tends to overestimate the values of the lifetimes other than those of the Y/B ratios, confirming at least its partial inadequacy in the assessment of the radiative properties and/or, second, the non-radiative processes in the investigated materials are very efficient and complex, in agreement with the non-exponential profiles of the decay curves, and dramatically reduce their quantum efficiencies. Further experimental and theoretical work is necessary in our opinion to make clarity on these interesting aspects of the still relatively unexplored spectroscopy of the Dy^{3+} ion.

4. Conclusions

The room-temperature optical spectra of the KYF and LiLuF single crystal fibers activated with Dy^{3+} have been measured and analyzed in the framework of the J–O approach. The relation between the intensity parameters of the theory, Ω_2 and Ω_4 in particular, and the relative intensities of the blue and yellow emission bands has been pointed out. This information can constitute an useful criterion to tailor the luminescence properties by a proper choice of the composition. In this perspective there are some points still to be clarified. It is evident for example that low values of the Ω_2 parameter imply relatively high values of the blue/yellow ratio and of the radiative lifetime. The results of the present work indicate, however, that the agreement between experimental and theoretical results is more qualitative than quantitative, and that further work is necessary to assess the effective role of the non-radiative processes.

Acknowledgments

References

[1] J. Limpert, H. Zellmer, P. Riedel, G. Maze, A. Tunnermann, Electron. Lett. 36 (2000) 1386.
[2] A. Kaminskii, U. Hömmerich, D. Temple, J.T. Seo, K. Ueda, S. Bagayev, A. Pavlyulk, Jpn. J. Appl. Phys. 39 (2000) L208.
[3] W.W. Holloway Jr., M. Kestigian, J. Opt. Soc. Am. 59 (1969) 60.
[4] R.-J. Xie, N. Hirosaki, M. Mitomo, K. Sakuma, N. Kimura, Appl. Phys. Lett. 89 (2006) 241103.
[5] B.R. Judd, Phys. Rev. 127 (1962) 750.
[6] G.S. Ofelt, J. Chem. Phys. 37 (1962) 511.
[7] N.P. Barnes, R.E. Allen, IEEE J. Quantum Electron. 27 (1991) 277.
[8] D. Parisi, A. Toncelli, M. Tonelli, E. Cavalli, E. Bovero, A. Belletti, J. Phys. Condens. Matter 17 (2005) 2783.
[9] K.J. Kim, A. Jouini, A. Yoshikawa, R. Simura, G. Boulon, T. Fukuda, J. Cryst. Growth 299 (2007) 171.
[10] A. Grzechnik, J. Nuss, K. Friese, J.-Y. Gesland, M. Jansen, Z. Krist. 217 (2002) 460.
[11] A.A. Kaminskii, K. Ueda, N. Uehara, Jpn. J. Appl. Phys. 32 (1993) L586.
[12] C.K. Jayasankar, E. Rukmini, Physica B 240 (1997) 273.
[13] I.R. Martín, Y. Guyotb, M.F. Joubertb, R. Yu. Abdulsabirovc, S.L. Korablevac, V.V. Semashkoc, J. Alloys Compd. 323–324 (2001) 763.
[14] R.D. Peacock, Struct. Bonding (Berlin) 22 (1975) 83.
[15] E. Cavalli, M. Bettinelli, A. Belletti, A. Speghini, J. Alloys Compd. 341 (2002) 107.
[16] R. Martinez Vazquez, R. Osellame, M. Marangoni, R. Ramponi, E. Dieguez, M. Ferrari, M. Matterelli, J. Phys. Condens. Matter 16 (2004) 465.
[17] A.A. Kaminskii, J.B. Gruber, S.N. Bagaev, K. Ueda, U. Hömmerich, J.T. Seo, D. Temple, B. Zandi, A.A. Kornienko, E.B. Dunina, A.A. Pavlyuk, R.F. Klevtsova, F.A. Kuznetsov, Phys. Rev. B 65 (2002) 125108.
[18] L. Macalik, J. Hanuza, B. Macalik, W. Ryba-Romanowski, S. Golab, A. Pietraszko, J. Lumin. 79 (1998) 9.
[19] E. Cavalli, E. Bovero, A. Belletti, J. Phys. Condens. Matter 14 (2002) 5221.
[20] L.W. Xu, H.M. Crosswhite, J.P. Hessler, J. Chem. Phys. 81 (1984) 698.
[21] S. Shionoya, W.M. Yen (Eds.), Phosphor Handbook, CRC Press, Boca Raton, USA, 1999, p. 104.
[22] G. Dominiak-Dzik, P. Solarz, W. Ryba-Romanowski, E. Beregi, L. Kovacs, J. Alloys Compd. 359 (2003) 51.